Journal of Biomolecular NMR, 6 (1995) 198–210
ESCOM

J-Bio NMR 284

^{1}H, ^{13}C and ^{15}N assignments and chemical shift-derived secondary structure of intestinal fatty acid-binding protein

Michael E. Hodsdon, James J. Toner and David P. Cistola*

Department of Biochemistry and Molecular Biophysics, Washington University School of Medicine, 660 South Euclid Avenue, Campus Box 8231, St. Louis, MO 63110-1010, U.S.A.

Received 9 January 1995
Accepted 21 March 1995

Keywords: Triple-resonance 3D NMR; Lipid-binding proteins; Isotope enrichment; Resonance assignments; Chemical shift; Protein secondary structure

Summary

Sequence-specific ^{1}H, ^{13}C and ^{15}N resonance assignments have been established for rat intestinal fatty acid-binding protein complexed with palmitate (15.4 kDa) at pH 7.2 and 37 °C. The resonance assignment strategy involved the concerted use of seven 3D triple-resonance experiments (CC-TOCSY, HCCH-TOCSY, HNCO, HNCA, ^{15}N-TOCSY-HMQC, HCACO and HCA(CO)N). A central feature of this strategy was the concurrent assignment of both backbone and side-chain aliphatic atoms, which was critical for overcoming ambiguities in the assignment process. The CC-TOCSY experiment provided the unambiguous links between the side-chain spin systems observed in HCCH-TOCSY and the backbone correlations observed in the other experiments. Assignments were established for 124 of the 131 residues, although 6 of the 124 had missing amide ^{1}H resonances, presumably due to rapid exchange with solvent under these experimental conditions. The assignment database was used to determine the solution secondary structure of the complex, based on chemical shift indices for the $^{1}H^{\alpha}$, $^{13}C^{\alpha}$, $^{13}C^{\beta}$ and ^{13}CO atoms. Overall, the secondary structure agreed well with that determined by X-ray crystallography [Sacchettini et al. (1989) *J. Mol. Biol.*, **208**, 327–339], although minor differences were observed at the edges of secondary structure elements.

Introduction

Intestinal fatty acid-binding protein (I-FABP) belongs to a family of soluble, intracellular proteins that are thought to facilitate the transport and trafficking of polar lipids (Glatz and Van der Vusse, 1990; Kaikaus et al., 1990; Veerkamp et al., 1991; Bass, 1993; Banaszak et al., 1994). This family includes at least 20 distinct fatty acid-, retinoid- and sterol-binding proteins which have been identified in a variety of vertebrate and invertebrate organisms. In mammals, different tissues within the same organism often express distinct lipid-binding proteins, implying that these proteins have functions that are tailored to the particular cell types in which they are found.

To date, three-dimensional structures have been determined for nine of the family members (Banaszak et al., 1994; Haunerland et al., 1994). Despite a variable degree of sequence identity, ranging from 19 to 64%, these structures exhibit essentially the same backbone fold. The root-mean-square (rms) differences for their α-carbon coordinates are 0.6 to 2.4 Å. In contrast, there are striking differences between the ligand-binding specificities for a number of these proteins. For example, I-FABP is specific for long-chain fatty acids, while cellular retinol-binding protein-II (CRBP-II) binds retinol and retinaldehyde, but not fatty acids. In addition, some proteins are able to discriminate between lipids within the same class, e.g., retinol versus retinal (Li et al., 1991). In spite of the substantial body of structural information for these proteins, the determinants of ligand-binding specificity and affinity in this protein family remain unclear.

The lipid-binding proteins from the small intestine are unusual in that several homologues are abundantly expressed in the same cell type, the enterocyte. In addition to I-FABP and CRBP-II, these homologues include liver

*To whom correspondence should be addressed.

fatty acid-binding protein and ileal lipid-binding protein*. Since the intestinal proteins exhibit distinct lipid-binding properties, they constitute a useful model system for investigating the determinants of lipid-binding specificity and affinity. Starting with I-FABP, we have begun a long-term project to establish a resonance assignment database for the lipid-binding proteins from intestine, as well as several mutant forms with altered ligand specificity (Jakoby et al., 1993). The assignments will facilitate a detailed comparison of the structural, dynamical, energetic and kinetic properties of these proteins in solution and the effect of bound ligand on these properties. In particular, it will permit a residue-specific interpretation and comparison of chemical shifts, NOEs, amide proton exchange rates, ^{15}N and ^{13}C relaxation rates and fractionation factors.

In this paper, we present sequence-specific ^{1}H, ^{13}C and ^{15}N resonance assignments for rat I-FABP complexed with palmitate (15.4 kDa). The assignments were established using a uniformly ^{13}C-/^{15}N-enriched protein and seven 3D triple-resonance experiments, and include nearly all of the backbone and aliphatic atoms of the side chains. In addition, we present the solution secondary structure of the complex, as determined from chemical shift indices for the $^{1}H^{\alpha}$, $^{13}C^{\alpha}$, ^{13}CO and $^{13}C^{\beta}$ atoms of each residue. The chemical shift-derived secondary structure is compared with that determined by X-ray crystallography (Sacchettini et al., 1989).

Materials and Methods

Protein biosynthesis and purification

Uniformly ^{13}C- and ^{15}N-enriched I-FABP was biosynthesized in *E. coli* MG-1655 using a two-stage strategy, designed to achieve an optimal balance between cell growth and isotope utilization. Bacteria harboring the pMON5840-I-FABP plasmid were grown at 37 °C in a New Brunswick Bioflo-III high-density fermentor, equipped with a 1.25 l vessel. In the first stage, a supplemented M9 medium (Li et al., 1987) was employed. Logarithmic growth was supported by periodic additions of non-isotope-enriched nutrients, totaling 12 g of glucose and 3 g ammonium chloride. At a cell density of ~ 13 OD_{600} units, the bacteria were harvested by centrifugation. In the second stage, the cells were resuspended in an otherwise identical medium containing 0.5 g [88%-U-^{13}C]-glucose (Isotec, Lot OU1687) and 4.0 g [99.5%-^{15}N]-ammonium chloride (Isotec, Lot OU0978). The resuspended cells were returned to the fermentor, and protein expression, under control of the recA promoter, was induced with nalidixic acid. Additional [^{13}C]-glucose was added in three separate aliquots during the second stage, and the total amount of [^{13}C]-glucose used during the fermentation was 7.6 g. During bacterial growth, the presence of glucose in the medium was monitored by the use of Diastix reagent strips (Miles, Inc., Elkhart, IN), the type used by diabetic subjects to monitor urinary glucose. Additionally, during the second stage, small aliquots of the culture were periodically removed for analysis using ^{13}C NMR. At ~ 1.5 h after induction, the [^{13}C]-enriched glucose was depleted and the cells were harvested. The final cell density was 21 OD_{600} units and the fermentation volume was ~ 1 l. The harvested cells were stored at −70 °C for further processing.

The protocols for protein purification and delipidation have been detailed elsewhere (Lowe et al., 1987; Jakoby et al., 1993). The final buffer composition was 20 mM potassium phosphate, 50 mM potassium chloride and 0.05% sodium azide at pH 7.2. The final yield of purified [^{13}C/^{15}N]-I-FABP from a single fermentation was 256 mg.

A portion of the delipidated, concentrated protein sample containing 20% D_2O was complexed with a stoichiometric amount of perdeuterated palmitic acid, as described by Cistola et al. (1989). The sample was divided into two equal aliquots. The first aliquot ('H_2O sample') was transferred to an ultra-thin-walled 545-PPT Wilmad NMR tube and stored at 4 °C prior to NMR data collection. A second, identical aliquot ('D_2O sample') was lyophilized, resuspended in 99.996% D_2O and similarly transferred to an NMR tube for storage. The protein concentration in the NMR samples was ~ 3 mM.

NMR spectroscopy

NMR spectra were collected at 37 °C using a Varian Unity-500 spectrometer equipped with a Nalorac 5 mm triple-resonance probe. One exception was the 3D CC-TOCSY spectrum, which was collected using a Varian Unity-600 spectrometer equipped with a Varian 5 mm triple-resonance probe. All experiments employed hypercomplex data aquisition to achieve quadrature detection in the indirectly detected dimensions (States et al., 1982). The aquisition parameters for each experiment are summarized in Table 1. Unless otherwise stated, GARP-1 (Shaka et al., 1985) and WALTZ-16 (Shaka et al., 1983) were used for broadband decoupling, and water suppression was achieved by using low-power presaturation (< 25 μW) of the HDO resonance. ^{1}H and ^{13}C chemical shifts were referenced to external sodium 3-(trimethylsilyl)-propionate-2,2,3,3-d_4 (TSP) in D_2O at 37 °C (0.0 ppm). Nitrogen chemical shifts were referenced to external $^{15}NH_4Cl$ (2.9 mM) in 1 M HCl at 37 °C (24.93 ppm relative to liquid NH_3; Levy and Lichter, 1979).

The two-dimensional ^{1}H-^{15}N HSQC pulse sequence (Bodenhausen and Ruben, 1980; Bax et al., 1990b) was modified to include a 1.5 ms purge pulse for water suppression at the end of the first INEPT subsequence

*Ileal lipid-binding protein has been alternatively referred to as gastrotropin, bile acid-binding protein, I-15P and intestinal fatty acid-binding protein-2.

TABLE I
AQUISITION PARAMETERS FOR NMR EXPERIMENTS ON I-FABP

Experiment	Nucleus			No. of complex points			Spectral width (kHz)			Scans	Total exp. time (h)
	F1	F2	F3	F1	F2	F3	F1	F2	F3		
HSQC	^{15}N	^{1}H		600	512		3.53	6.50		32	18
HNCO	^{13}CO	^{15}N	$^{1}H^{N}$	34	34	256	2.20	2.20	6.50	128	59
HNCA	^{13}C	^{15}N	$^{1}H^{N}$	46	31	256	3.30	2.20	6.50	128	71
^{15}N-TOCSY	^{1}H	^{15}N	$^{1}H^{N}$	170	39	256	6.50	2.20	6.50	24	190
HCACO	$^{13}C^{\alpha}$	^{13}CO	$^{1}H^{\alpha}$	24	40	256	3.30	2.20	6.50	64	61
HCA(CO)N	$^{13}C^{\alpha}$	^{13}CO	$^{1}H^{\alpha}$	24	44	256	3.30	2.20	6.50	64	67
CC-TOCSY	^{13}C	^{13}CO	$^{1}H^{\alpha}$	50	39	256	9.40	2.60	7.80	64	156
HCCH-TOCSY	^{1}H	^{13}C	^{1}H	128	32	256	3.80	2.60	3.80	16	76

(Messerle et al., 1989). Delay values of 2.3 ms ($1/4J_{NH}$) were used during both INEPT subsequences. The total relaxation delay was 1.5 s, and no water presaturation was employed during this experiment.

Three-dimensional HNCO and HNCA experiments (Kay et al., 1990) were performed using pulse sequences optimized to include modified INEPT subsequences (Farmer et al., 1992). Because of hardware limitations, no broadband ^{1}H decoupling was employed in the period between INEPT transfers; instead, 180° refocusing pulses were used to decouple ^{1}H during the ^{15}N evolution period (t_2). With the ^{13}C carrier frequency centered on the carbonyl carbon region, excitation of α-carbons was achieved by the use of frequency-shifted laminar pulses (Patt, 1992). The delay values used during the modified INEPT subsequences were 5.0 and 5.3 ms (5–10% shorter than $1/2J_{NH}$) for HNCO and HNCA, respectively. In order to establish ^{15}N-^{13}C multiple-quantum coherence, delay values of 27.8 ms (~17% shorter than $1/2J_{CO\text{-}N}$) and 35.7 ms (~28% shorter than $1/2J_{C\alpha N}$) were used for the same respective experiments.

The three-dimensional ^{15}N-TOCSY-HMQC experiment

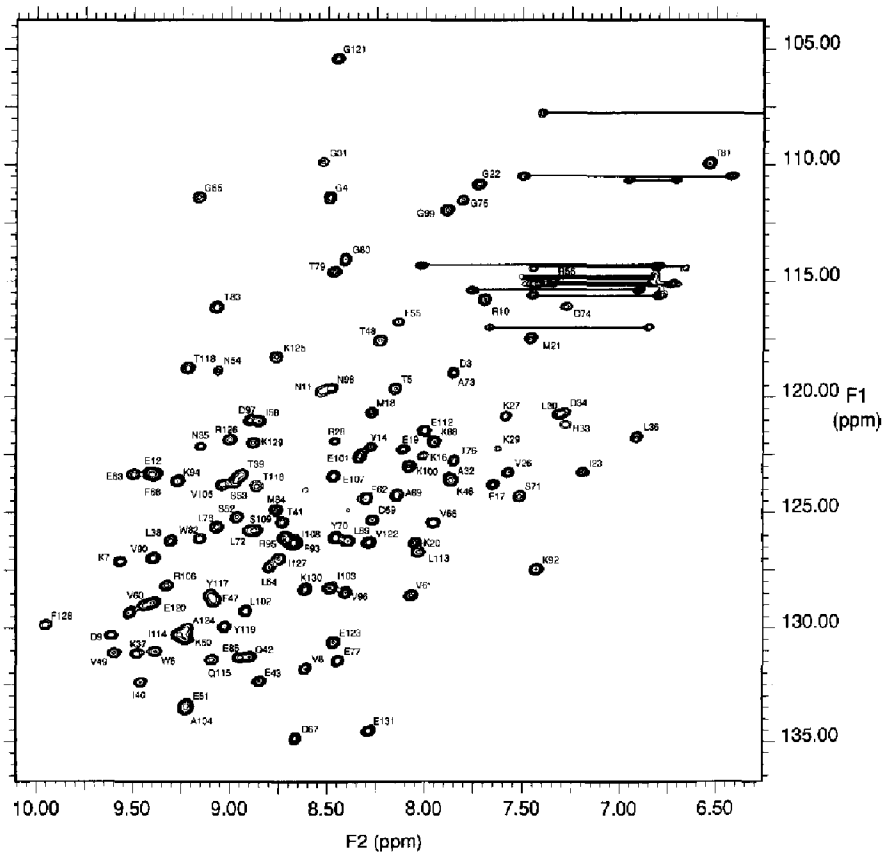

Fig. 1. Two-dimensional ^{1}H-^{15}N HSQC spectrum of uniformly ^{13}C-/^{15}N-enriched I-FABP complexed with perdeuterated palmitate. The sample concentration was 3 mM, pH 7.2, 37 °C. Backbone amide correlations are labeled according to the assignments described in the text and are listed in Table 3. The horizontal lines indicate the correlations between the NH_2 protons in asparagine and glutamine side chains.

TABLE 2
PROCESSING PARAMETERS FOR NMR EXPERIMENTS ON I-FABP

Experiment	Exponential factor			Gaussian factor			No. of processed real points		
	F1	F2	F3	F1	F2	F3	F1	F2	F3
HSQC	–4	–4		0.070	0.050		1024	1024	
HNCO	–5	–5	–5	0.020	0.010	0.030	64	64	256
HNCA	–	–5	–5	0.030	0.015	0.030	64	64	256
^{15}N-TOCSY	–	–	10	0.037	0.037	–	256	64	256
HCACO	10	10	5	0.007	0.020	0.028	64	64	256
HCA(CO)N	10	5	5	0.010	0.020	0.028	64	64	256
CC-TOCSY	10	–	15	0.006	0.016	–	64	64	256
HCCH-TOCSY	5	–10	5	–	0.01	–	256	64	512

(Marion et al., 1989) was performed with a 90 ms MLEV-17 spin-lock, preceded by a 2.0 ms nonselective trim pulse. A delay of 4.5 ms, ~20% shorter than $1/2J_{NH}$, was used to establish antiphase magnetization prior to the generation of ^{1}H-^{15}N multiple-quantum coherence.

The α-proton-detected spectra were collected using the D_2O sample. These experiments included the constant-time versions of three-dimensional HCACO and HCA(CO)N (Powers et al., 1991) and CC-TOCSY (Kay, 1993). During the INEPT subsequences, delay values of 1.8 ms (~10% less than $1/4J_{CH}$) were used. The total duration of the constant-time period ($t_1 = 1/J_{CH}$) was 7.4 ms for HCACO and HCA(CO)N and 6.0 ms for CC-TOCSY. The delay in the HCA(CO)N experiment just prior to the generation of ^{13}CO-^{15}N multiple-quantum coherence was 24 ms, ~27% less than $1/2J_{CN}$. In the CC-TOCSY experiment, a 3.6 ms delay ($1/2J_{C\alpha CO}$) was used during the polarization transfer between $^{13}C^{\alpha}$ and ^{13}CO. Except for CC-TOCSY, the ^{13}C carrier frequency was centered on the α-carbons (53 ppm). For CC-TOCSY, the ^{13}C carrier frequency was initially centered at 39 ppm during the initial INEPT subsequence to cover the side-chain aliphatic carbons. For the remainder of the pulse sequence, it was shifted to 53 ppm. Excitation of carbonyl carbons was achieved using frequency-shifted laminar pulses. The carbon pulse widths were selected so that minimal excitation occurred in the α-carbon region (Kay et al., 1992).

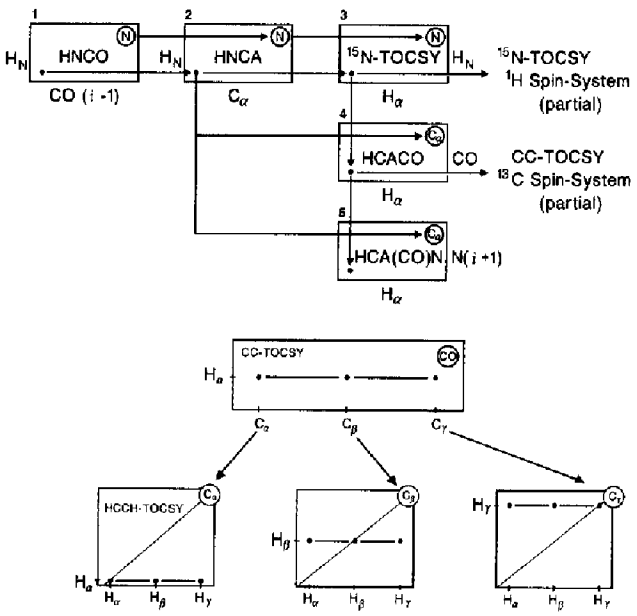

Fig. 2. Strategy used for establishing sequence-specific ^{1}H, ^{13}C and ^{15}N resonance assignments for the backbone and side-chain (aliphatic) atoms of I-FABP. Each box represents a 2D plane from a 3D spectrum, and the axis for the third dimension is circled in the upper right-hand corner. The top of the figure shows the five 3D spectra used for sequential correlation of the backbone atoms. Unless otherwise designated, the atoms represent those of residue i. Partial ^{1}H and ^{13}C spin systems found in ^{15}N-TOCSY and CC-TOCSY, respectively, were directly and unambiguously correlated to the backbone atoms. As shown in the lower part of the figure, side-chain atom assignments could then be completed using multiple ^{13}C spectral planes from the 3D HCCH-TOCSY spectrum.

The three-dimensional HCCH-TOCSY pulse sequence (Bax et al., 1990a) was modified to require only two radiofrequency channels, and the ^{13}C carrier frequency was centered at 45 ppm. A frequency-shifted, laminar Hermitian 180° pulse was used to decouple carbonyl carbons during t_2. The width of this 180° pulse was chosen so as to minimize excitation of the aliphatic carbons (Bax et al., 1990a). For ^{13}C isotropic mixing and polarization transfer, a 23.4 ms DIPSI-3 subsequence (Shaka et al., 1988) was employed. The delay values for both INEPT subsequences were 1.6 ms (~20% less than $1/4J_{CH}$).

NMR processing and data analysis

Initial processing of the time-domain spectra was performed on a Sun SPARC-2 workstation using VNMR v. 4.2 (Varian Associates). The parameters used for apodization and zero-filling are summarized in Table 2. The processed and phased frequency-domain spectra ('phase-files' in VNMR) were then imported into NMR COMPASS v. 2.0 (Molecular Simulations, Inc.) running on a Silicon Graphics 4D-25TG workstation. Assignments were established in a computer-assisted manner by simultaneous display and manipulation of multiple spectra, as detailed below.

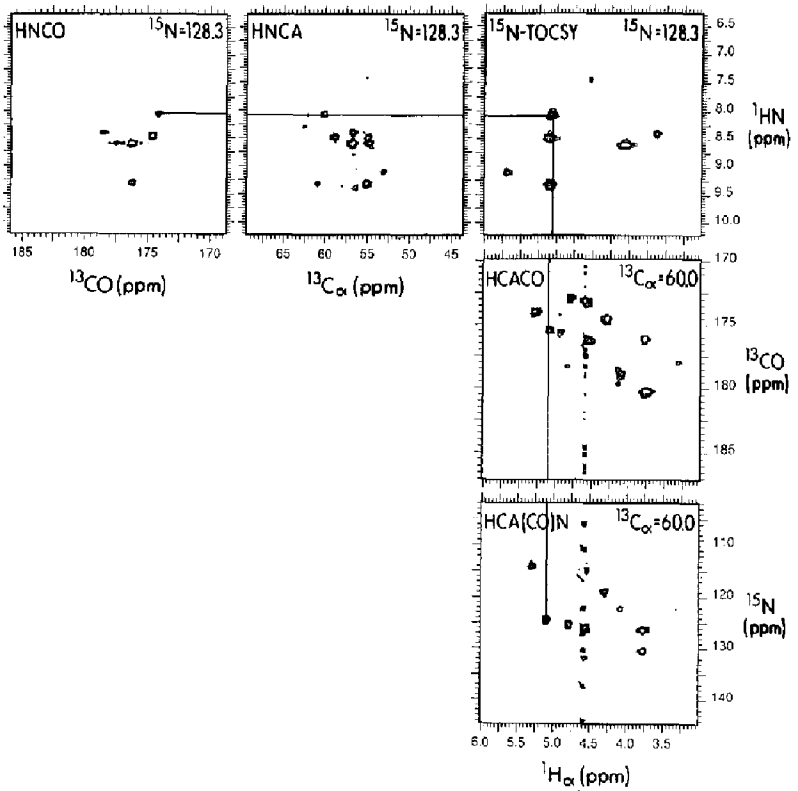

Fig. 3. Backbone atom correlations for residue Val[61]. Correlations between peaks in the five spectral planes displayed map the chemical shifts of all backbone atoms in this residue and, as well, provide important interresidue correlations necessary for sequential assignment.

Results and Discussion

Two-dimensional HSQC

The ^{1}H-^{15}N HSQC spectrum of ^{13}C-/^{15}N-enriched I-FABP displayed excellent sensitivity and chemical shift dispersion, allowing easy identification of most of the NH correlations. This spectrum, obtained at pH 7.2 without water presaturation, showed 123 out of the possible 131 backbone cross peaks (Fig. 1). Of these 123, 118 were assigned using the 3D methods described below.* Four of the five unassigned cross peaks observed in the HSQC spectrum were significantly lower in intensity than the others. Because the HSQC experiment exhibited a higher sensitivity and employed a single purge pulse for water suppression, it could be expected to detect a higher number of amide correlations than the less sensitive 3D experiments that employed low-power presaturation of the water resonance.

Also seen in Fig. 1 are 12 pairs of correlated peaks, connected by horizontal lines. These represent the 10 asparagine and two glutamine side-chain NH_2 groups in I-FABP. Not shown are two ^{1}H/^{15}N correlations that were observed at 10.20/126.3 and 10.72/134.7 ppm.

Assignment strategy and rationale

Although two-dimensional NMR spectra of I-FABP showed good sensitivity and resolution, the added correlative information of three-dimensional spectroscopy was necessary for the unambiguous assignment of this 15.4-kDa complex. The complete assignment strategy involved the concerted use of seven 3D NMR experiments, as diagrammed in Fig. 2. Five of the seven experiments were used to correlate backbone atoms, as shown in the upper panel of the figure. These five experiments are nearly identical to those used by Ikura et al. (1990) for the backbone assignment of calmodulin. For I-FABP, we employed two additional experiments, HCCH-TOCSY and CC-TOCSY, as well as a long-mixing-time version of ^{15}N-TOCSY, to correlate backbone with side-chain atoms. For reasons explained below, these additional experiments were critically important for the unambiguous assignment of the protein backbone.

Our initial approach was to employ the five backbone triple-resonance experiments supplemented only with side-chain correlations from HCCH-TOCSY. However, for I-FABP, several sources of ambiguity were encountered during the assignment process. First, glycine residues did

*For one residue (Glu[15]), there was no observable peak in the 2D HSQC spectrum corresponding to the assigned amide ^{1}H and ^{15}N, resulting in some degree of uncertainty in this assignment. This was the only residue whose backbone atom assignments appeared complete, but for which no corresponding side-chain resonances were identified.

not produce observable correlations in HCACO and HCA(CO)N spectra, presumably because of rapid transverse relaxation. These missing correlations, along with the 13 missing amide proton resonances, caused breaks in the essentially linear process of assigning the backbone atoms. Moreover, the frequent occurrence of multiple possible correlations between the sometimes crowded 3D spectral planes severely limited the maximum number of adjacent correlated residues that could be assigned. Unambiguously assigned stretches of backbone atoms were rarely longer than four or five residues, and typically contained only three or four residues.

Contributing to this problem were limitations experienced in the initial use of the HCCH-TOCSY experiment for assignment of the side-chain resonances. Proton spin systems in the HCCH-TOCSY are correlated to the backbone atom assignments through the $^{13}C^{\alpha}$ and $^{1}H^{\alpha}$ dimensions. For I-FABP, correlations in this region of the spectrum generally showed low sensitivity and poor chemical shift dispersion. Although the same ^{1}H spin systems were also found with higher sensitivity and better resolution in HCCH-TOCSY planes corresponding to other side-chain carbons, this information could not be utilized without a means for connecting the backbone atoms with their side-chain carbons.

To overcome these problems, two modifications were made to the original assignment strategy of Ikura et al. (1990). The first was to utilize the ^{13}C spin systems found in the CC-TOCSY spectrum. Besides providing an additional determination of the amino acid type for each residue, the ^{13}C spin systems yielded the information required to choose the appropriate ^{13}C spectral planes in the HCCH-TOCSY experiment. In effect, this made the HCCH-TOCSY experiment much more powerful for obtaining unambiguous and redundant proton side-chain assignments and for connecting side-chain and backbone atoms. The concerted use of CC-TOCSY and HCCH-TOCSY is illustrated in the lower panel of Fig. 2.

The second modification simply involved the collection of a ^{15}N-TOCSY-HMQC spectrum with a longer mixing time, in order to further correlate the ^{1}HN, ^{15}N and $^{1}H^{\alpha}$ with the side-chain ^{1}H resonances. The advantage of using the ^{15}N-TOCSY experiment for side-chain assignments is twofold: the near absence of degenerate ^{1}HN and ^{15}N chemical shifts and the unambiguous correlation of the ^{1}H side-chain resonances to the backbone amide atoms. In a similar manner, the CC-TOCSY experiment is essentially an HCACO experiment with the $^{13}C^{\alpha}$ dimension replaced by a full ^{13}C spectral window. It also provides the same direct relationship between the carbon side-chain atoms and the backbone ^{13}CO, $^{13}C^{\alpha}$ and $^{1}H^{\alpha}$.

The connection between the three ^{1}HN-detected experiments and the HCACO and HCA(CO)N spectra represented a weak link in the cycle of correlation between backbone atoms. This occurred primarily because the $^{13}C^{\alpha}$ and $^{1}H^{\alpha}$ dimensions, which tie the two sets of spectra, exhibited poor chemical shift dispersion. In a sense, by comparing the side-chain resonances found in the ^{15}N-TOCSY and the CC-TOCSY/HCCH-TOCSY spectra, the side-chain atom assignments served as an additional constraint on the cycle of backbone atom correlations. Due to this relationship, the side-chain atom assignments represented an integral, rather than supplementary, part of the modified assignment strategy.

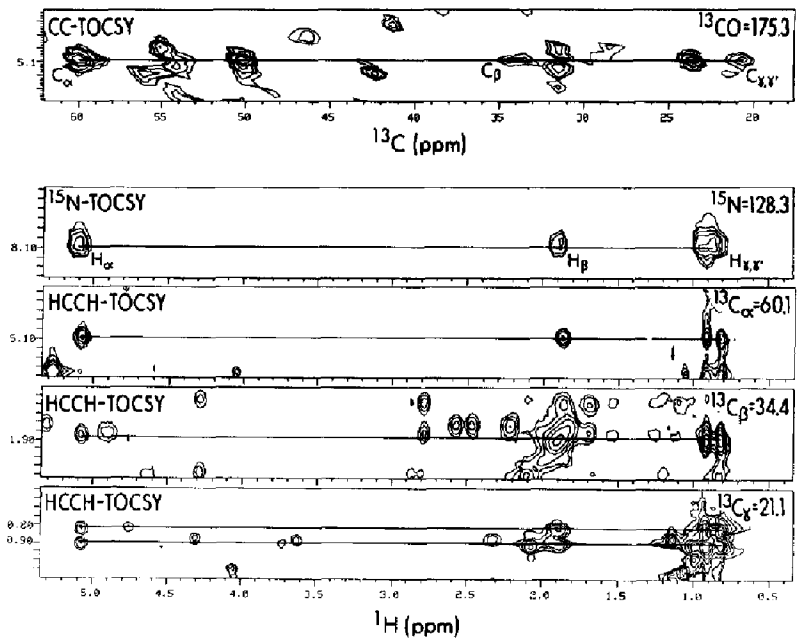

Fig. 4. Side-chain/backbone atom correlations for residue Val[61]. The top panel shows a CC-TOCSY plane with the ^{13}C side-chain resonances for Val[61] labelled. Below, the ^{1}H assignments for this residue are shown in the ^{15}N-TOCSY-HMQC spectrum. This ^{1}H spin system can also be found in the three HCCH-TOCSY spectral planes representing the C^{α}, C^{β} and C^{γ} of Val[60].

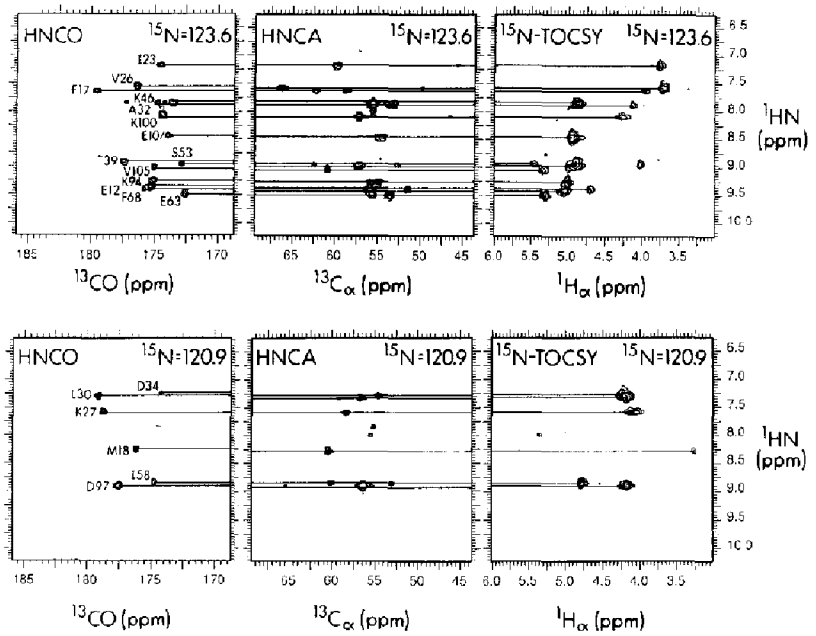

Fig. 5. Two sets of ^{15}N planes from the ^{1}HN-detected experiments, i.e., HNCO, HNCA and ^{15}N-TOCSY-HMQC. The horizontal lines illustrate correlations between backbone atoms for various residues of I-FABP.

Assignment cycle for Val^{61}

To illustrate the use of this strategy, the assignments for residue Val^{61} are described in detail. Figure 3 shows one cycle of backbone atom correlations for this residue, as well as correlations to residues 60 and 62. The horizontal line in Fig. 3 represents a set of cross peaks that share the same amide proton (8.09 ppm) and nitrogen (128.3 ppm) chemical shifts. In practice, such correlations were established by displaying all three spectra simultaneously and tying their y- and z-axes together using NMR COMPASS. Because only one set of cross peaks fell on this line, the correlation was unambiguous. The x-axis value from the HNCO spectrum (174.2 ppm) provided the carbonyl chemical shift of residue 60. In the HNCA spec-

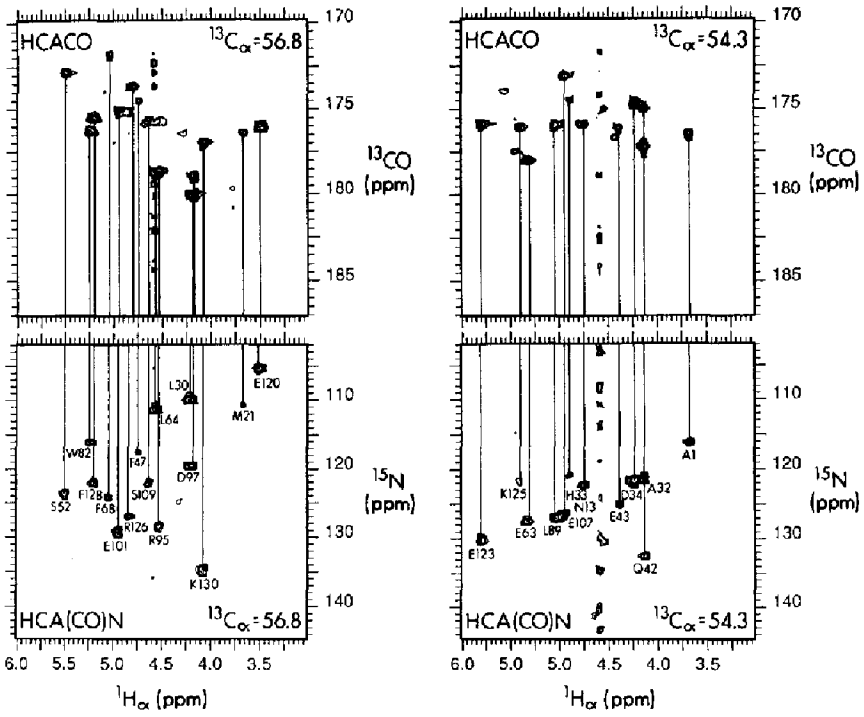

Fig. 6. Two sets of $^{13}C^{\alpha}$ planes from the $^{1}H^{\alpha}$-detected experiments, i.e., HCACO and HCA(CO)N. The vertical lines illustrate correlations between backbone atoms for various residues.

trum, two cross peaks were observed along this line. The more intense peak at 60.0 ppm represented the intraresidue correlation for residue 61, and the less intense peak at 62.1 ppm indicated the interresidue correlation to the α-carbon of residue 60. The latter provided an additional constraint on the connection to residue 60. In many cases, such interresidue HNCA correlations were critically important for resolving ambiguities in sequential connections.

The chemical shift of the intraresidue α-carbon (60.0 ppm) was used to determine the corresponding α-carbon planes in the HCACO and HCA(CO)N experiments. The x-axes of the ^{15}N-TOCSY, HCACO and HCA(CO)N experiments were then tied together, and a set of cross peaks was correlated by the vertical line at an α-proton chemical shift of 5.05 ppm, as shown in Fig. 3. At first sight, it may appear that two additional cross peaks in the ^{15}N-TOCSY spectrum, at amide ^{1}H values of 8.5 and 9.3 ppm, may also be associated with this vertical line. However, these cross peaks correspond to residues that have different α-carbon chemical shifts and, therefore, to peaks that appear in HCACO and HCA(CO)N planes different from those shown in Fig. 3.

The vertical axes from the HCACO and HCA(CO)N spectra provided the carbonyl chemical shift of residue 61 (175.3 ppm) and the amide nitrogen shift of residue 62 (124.3 ppm), respectively. The latter was then used to choose the next nitrogen plane for the top three spectra in order to begin the next assignment cycle.

The integration of backbone and side-chain assignments for this assignment cycle is illustrated in Fig. 4. Side-chain ^{1}H assignments for residue 61 were first observed in the ^{15}N-TOCSY spectrum (second panel from the top). The same ^{1}H spin system, corresponding to a valine, was also found in three different planes of the HCCH-TOCSY spectrum. These HCCH-TOCSY carbon planes were selected on the basis of the ^{13}C side-chain resonances identified in the CC-TOCSY spectrum and correspond to the α- (60.0 ppm), β- (34.4 ppm), γ and γ'-carbons (21.1 ppm) of Val^{61}.

In the CC-TOCSY plane shown in Fig. 4, note that the carbon spin system for Val^{61} directly overlaps with that for Ala^{104}. The presence of ^{13}C spin systems degenerate in both their ^{13}CO and ^{1}H$^{\alpha}$ chemical shifts was an occasional source of ambiguity. However, this ambiguity was easily overcome with the concerted use of the HCCH-TOCSY spectrum, as described above.

Additional examples

Backbone atom correlations for I-FABP are presented for two sets of spectral planes in the ^{1}HN-detected experiments (Fig. 5) and the H$^{\alpha}$-detected experiments (Fig. 6). The planes at the top of Fig. 5 are among the most crowded that we observed. Note that some of these correlations may not actually have their peak maxima located in the spectral planes displayed; they are visible because of their large line widths and the coarse digitization employed in the third dimension.

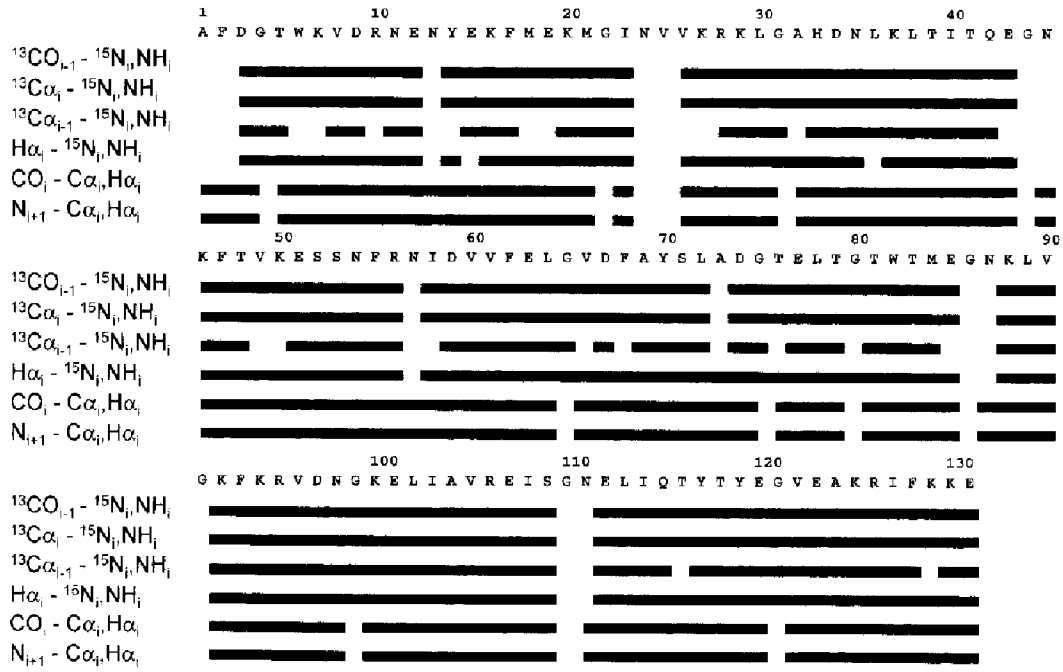

Fig. 7. Schematic representation of the continuity of triple-resonance spectral correlations used for assignment of the backbone resonances. The presence of a correlation peak for a residue is represented by a horizontal bar, whereas the gaps denote the absence of a correlation. The correlations are expressed with respect to the proton which is directly detected in the experiment on the far right, the directly attached heteronucleus to its immediate left and the second correlated heteronucleus on the far left. Starting from the top, the correlations listed are found in the HNCO, HNCA (intraresidue), HNCA (interresidue), ^{15}N-TOCSY-HMQC, HCACO and HCA(CO)N spectra.

TABLE 3
BACKBONE ASSIGNMENTS (ppm) FOR I-FABP[a]

Residue	^{15}N	H^N	$^{13}C^\alpha$	H^α	^{13}CO	Residue	^{15}N	H^N	$^{13}C^\alpha$	H^α	^{13}CO
A1			52.7	3.83	176.9	D67	135.1	8.65	55.5	4.79	175.8
F2	119.5		59.6	4.28	174.4	F68	123.6	9.41	55.9	5.05	171.7
D3	118.8	7.84	55.1	4.54	176.7	A69	124.3	8.14	50.6	5.10	176.7
G4	111.4	8.50	44.0	4.03, 3.62	171.7	Y70	126.3	8.45	57.6	4.69	172.8
T5	119.5	8.14	62.5	5.15	172.6	S71	124.3	7.54	55.9	5.00	174.5
W6	131.0	9.36	55.1	5.15	175.3	L72	125.6	8.90	54.7	3.93	179.9
K7	127.0	9.57	54.7	5.30	176.7	A73	119.5	7.89	54.7	3.67	176.4
V8	131.7	8.60	65.0	3.17	173.1	D74	116.1	7.28	53.5	4.28	176.4
D9	130.4	9.62	55.5	4.89	175.3	G75	111.4	7.79	44.7	4.23, 3.42	174.7
R10	116.1	7.69	55.1	4.64	172.6	T76	122.9	7.84	65.0	3.78	173.9
N11	119.5	8.55	51.4	5.45	175.3	E77	131.7	8.45	57.2	4.49	175.8
E12	123.6	9.41	55.9	4.69	175.8	L78	125.6	9.06	53.5	5.40	177.5
N13	125.6		54.7	4.74	175.8	T79	114.8	8.45	60.0	5.25	173.9
Y14	122.2	8.30	59.2	4.54	177.5	G80	114.1	8.40	46.9	3.98, 3.83	170.1
E15[b]	122.9	8.91	56.4	4.03	179.1	T81	110.0	6.52	60.0	4.54	173.1
K16	122.9	7.99	58.4	4.03	179.4	W82	126.3	9.16	56.3	5.20	176.4
F17	123.6	7.64	62.1	3.93	176.1	T83	116.1	9.06	60.9	4.59	172.6
M18	120.9	8.30	60.5	3.27	178.0	M84	124.9	8.75	54.7	5.30	175.8
E19	122.2	8.09	60.0	3.73	180.2	E85	131.7	8.96	55.1	4.59	176.7
K20	126.3	8.04	57.6	4.08	178.8	G86					
M21	117.5	7.48	66.3	3.67	176.4	N87			53.1	4.84	174.5
G22	110.7	7.74	45.7	3.93, 3.62	174.5	K88	121.5	7.94	55.5	5.00	174.7
I23	123.6	7.18	60.0	3.78	176.1	L89	126.3	8.40	53.9	5.00	175.8
N24	130.4					V90	127.0	9.41	62.5	4.74	175.0
V25						G91	126.3	10.17	44.9	4.54, 1.98	174.7
V26	123.6	7.59	66.2	3.73	178.8	K92	127.7	7.43	55.1	4.54	175.0
K27	120.9	7.59	58.4	4.08	178.6	F93	126.3	8.65	55.9	5.20	175.0
R28	122.2	8.45	59.2	4.08	178.8	K94	123.6	9.26	55.1	5.00	177.2
K29	122.2	7.64	59.2	4.08	179.1	R95	126.3	8.70	56.8	4.49	178.6
L30	120.9	7.33	56.8	4.18	179.9	V96	128.3	8.40	65.4	3.62	177.5
G31	110.0	8.50	47.3	3.98, 3.73	174.7	D97	120.9	8.91	56.3	4.18	178.8
A32	123.6	7.89	53.9	4.13	177.2	N98	119.5	8.50	51.4	4.79	177.5
H33	121.5	7.28	54.7	4.89	174.2	G99	112.0	7.89	46.5	4.03, 3.88	174.5
D34	120.9	7.28	54.7	4.23	176.7	K100	122.9	8.09	57.2	4.28	176.4
N35	122.2	9.16	53.9	4.23	174.7	E101	122.2	8.35	56.3	4.94	175.0
L36	121.5	6.93	57.2	4.39	175.0	L102	129.0	8.91	55.1	5.20	174.7
K37	131.0	9.47	55.1	5.55	175.0	I103	128.3	8.50	58.8	5.10	175.3
L38	126.3	9.31	52.7	5.55	177.5	A104	133.8	9.21	49.8	5.86	175.0
T39	123.6	8.96	62.5	5.45	174.7	V105	123.6	9.06	60.9	5.35	176.1
I40	132.4	9.47	61.3	4.94	175.8	R106	128.3	9.31	55.1	5.10	173.9
T41	125.6	8.75	61.3	4.64	172.6	E107	123.6	8.45	54.3	4.94	173.1
Q42	131.0	8.91	54.7	4.13	175.0	I108	126.3	8.65	58.4	4.79	176.9
E43	132.4	8.86	54.7	4.39	176.1	S109	125.6	8.86	56.3	4.64	175.5
G44						G110					
N45			53.1	4.79	173.7	N111			53.1	4.84	174.2
K46	123.6	7.84	55.5	4.89	174.7	E112	121.5	7.99	55.5	5.35	173.9
F47	129.0	9.06	56.3	4.74	174.5	L113	127.0	8.04	53.9	4.54	175.0
T48	117.5	8.25	62.1	4.74	173.7	I114	130.4	9.26	61.3	4.54	176.4
V49	131.0	9.62	61.3	4.64	175.3	Q115	131.7	9.11	54.3	5.55	173.9
K50	131.0	9.21	55.5	5.00	175.3	T116	124.3	8.86	61.3	4.89	173.9
E51	133.8	9.21	55.5	4.84	175.0	Y117	128.3	9.11	53.1	5.71	175.8
S52	125.6	8.96	56.8	5.50	172.8	T118	118.8	9.21	62.1	5.61	174.5
S53	123.6	8.96	57.2	4.89	174.5	Y119	129.7	9.01	58.0	4.84	173.7
N54	118.8	9.06	54.7	4.44	176.7	E120	129.0	9.41	56.3	3.47	176.1
F55	116.8	8.14	59.6	4.49	176.4	G121	105.2	8.45	45.7	4.03, 3.52	174.2
R56	115.4	7.33	55.5	4.69	172.6	V122	126.3	8.30	62.6	4.18	173.7
N57	119.5		53.1	5.91	174.7	E123	130.4	8.45	54.3	5.76	175.8
I58	120.9	8.86	60.0	4.79	172.8	A124	130.4	9.21	50.6	5.05	175.6
D59	125.6	8.25	53.5	5.45	175.6	K125	118.1	8.75	54.7	5.40	176.1
V60	129.0	9.47	62.1	4.28	174.2	R126	121.5	9.01	56.3	4.84	173.7
V61	128.3	8.09	60.0	5.05	175.3	I127	127.0	8.75	51.3	4.94	175.0
F62	124.3	8.30	55.5	4.84	172.6	F128	129.7	9.97	56.3	5.20	175.6
E63	123.6	9.52	53.5	5.30	178.0	K129	122.2	8.91	54.7	5.25	176.4
L64	127.7	8.81	56.8	4.54	178.6	K130	128.3	8.60	56.8	4.08	176.9
G65	111.4	9.16	46.1	4.23, 3.52	173.9	E131	134.4	8.30	58.4	4.08, 3.98	181.3
V66	125.6	7.94	62.5	4.28	176.4						

[a] The H^α chemical shifts of the following residues exhibited a +0.05 ppm isotope shift in D_2O: 5, 7, 9, 10, 16–19, 37, 39, 48, 50, 51, 53, 55, 61, 66, 71, 72, 77–79, 82, 84, 89, 90, 93, 95, 103, 104, 123 and 124. The values reported in the table are in H_2O.

[b] The assignments for Glu^{15} are tentative (see footnote on page 202).

TABLE 4
SIDE-CHAIN ^{1}H ASSIGNMENTS (ppm) FOR I-FABP

Residue	H^{β}	H^{γ}	$H^{\gamma'}$	H^{δ}	$H^{\delta'}$	H^{ε}
A1	1.37					
F2	3.10, 2.89					
D3	2.59, 2.50					
G4						
T5	3.83	1.08				
W6	2.83, 3.01					
K7	1.76, 1.95	1.49		1.67, 1.77		2.95
V8	1.65	0.25	0.90			
D9	2.51, 2.47					
R10	1.78	1.32, 1.56		3.11		
N11	2.56, 2.84					
E12	2.05, 2.13	1.78, 1.99				
N13	2.74, 3.82					
Y14	2.93					
E15						
K16	1.52, 1.75	1.36, 1.42		1.66		2.80
F17	3.12, 3.34					
M18	2.08	1.70				
E19	1.92, 2.14	1.99, 2.20				
K20	1.52, 1.75	1.36, 1.42		1.42, 1.66		2.80
M21	1.06, 1.25	1.45, 1.75				
G22						
I23	1.33	1.00, 1.30	0.78	0.46		
N24						
V25						
V26	2.05	0.90	0.99			
K27	1.53,1.75	1.34, 1.42		1.42, 1.65		2.80
R28	1.61, 1.87	1.35, 1.67		2.95, 3.05		
K29	1.76, 1.31	1.47, 1.55		1.66		2.91
L30	1.46, 1.80	1.64		0.73	0.87	
G31						
A32	1.27					
H33	2.78, 3.22					
D34	2.85					
N35	2.61, 3.04					
L36	1.65, 1.85	1.45		1.11	0.88	
K37	1.73, 1.85	1.39, 1.48		1.61		2.86
L38	1.07, 1.60	1.48		0.28	0.88	
T39	4.03	1.14				
I40	2.23	0.93, 1.70	0.75	0.54		
T41	3.85	1.06				
Q42	0.90	1.76				
E43	1.67, 1.83	1.95				
G44						
N45	2.90, 3.03					
K46	1.67, 1.85	1.10, 1.26		1.54		2.78
F47	1.03, 1.50					
T48	3.87	0.98				
V49	2.11	0.83	0.83			
K50	1.72, 1.87	1.24, 1.47		1.54		2.88
E51	1.96, 2.08	2.08, 2.25				
S52	3.80, 3.90					
S53	2.45, 2.53					
N54	2.57, 3.10					
F55	2.70, 3.23					
R56	1.78	1.34, 1.56		3.12		
N57	2.74					
I58	1.86	1.58	0.87	0.82		
D59	2.32, 2.56					
V60	2.31	1.14	1.19			
V61	1.86	0.82	0.91			
F62	2.83					
E63	1.83, 1.93	2.18				
L64	1.66, 1.99	2.11		1.14	0.74	
G65						
V66	2.30	0.88	1.14			
D67	2.41, 2.47					
F68	3.32, 3.57					
A69	1.44					
Y70	2.04, 3.04					
S71	3.42, 3.35					
L72	1.38, 2.12	1.65		0.76	0.64	
A73	0.78					
D74	1.90, 2.84					
G75						
T76	3.92	0.93				
E77	1.84, 2.07	2.07, 2.28				
L78	1.37, 1.69	1.55		0.59	0.45	
T79	4.03	1.05				
G80						
T81	3.68	0.92				
W82	2.44, 2.49					
T83	4.16	1.17				
M84	1.82, 2.20	2.46, 2.57				
E85	1.80, 1.93	2.10				
G86						
N87	2.89, 3.10					
K88	1.74, 1.86	1.38, 1.49		1.54		2.87
L89	0.83, 1.10	0.99		−0.17	−0.52	
V90	1.92	0.92	0.82			
G91						
K92	1.41, 1.52	1.08, 1.22		1.52		2.77
F93	2.67, 2.80					
K94	1.54	1.23		1.54		2.89
R95	2.11, 2.50	1.14, 1.69		2.80, 3.56		
V96	1.93	0.90	0.90			
D97	2.70, 2.79					
N98	2.88, 3.09					
G99						
K100	1.69, 2.10	1.21		1.43, 1.54		2.80, 2.87
E101	1.96	2.08, 2.26				
L102	1.49, 1.59	1.76		0.85	0.67	
I103	1.87	1.25, 1.53	0.87	0.81		
A104	1.14					
V105	1.98	0.98	0.98			
R106	1.14	1.13, 1.33		1.48, 1.77		
E107	1.84, 2.00	1.94, 2.10				
I108	1.60	0.98	0.76	0.37		
S109	3.46, 3.70					
G110						
N111	2.91, 3.03					
E112	1.96, 2.11	2.23, 2.41				
L113	−0.17, −0.23	0.78		−0.01	−0.42	
I114	1.80	1.11, 1.46	0.73	0.81		
Q115	1.83, 1.93	1.83, 2.06				
T116	3.80	1.10				
Y117	1.80, 2.67					
T118	3.97	1.14				
Y119	2.56, 3.06					
E120	1.34, 1.92	0.86, 1.41				
G121						
V122	2.35	0.97	0.97			
E123	1.91	1.95, 2.16				
A124	1.34					
K125	1.44	1.37		1.35, 1.46		2.79
R126	1.39, 1.46	1.33		2.47		
I127	2.23	0.94, 1.69	0.75	0.54		
F128	3.03, 3.34					
K129	1.90, 1.98	1.48, 1.64		1.73		2.97
K130	1.26, 1.42	0.20, 0.93		1.13, 1.19		2.60
E131	1.61, 1.85	2.05				

TABLE 5
SIDE-CHAIN ^{13}C ASSIGNMENTS (ppm) FOR I-FABP

Residue	C^{β}	C^{γ}	$C^{\gamma'}$	C^{δ}	$C^{\delta'}$	C^{ε}	Residue	C^{β}	C^{γ}	$C^{\gamma'}$	C^{δ}	$C^{\delta'}$	C^{ε}
A1	20.5						D67	42.2					
F2	40.2						F68	41.9					
D3	42.0						A69	21.6					
G4							Y70	43.2					
T5	70.3	22.1					S71	64.8					
W6	31.8						L72	42.8	28.3		24.8	24.9	
K7	36.4	24.8		29.6		42.2	A73	17.9					
V8	31.8	22.8	17.0				D74	41.2					
D9	47.0						G75						
R10	32.4	26.9		43.4			T76	67.6	20.6				
N11	43.7						E77	31.7	36.9				
E12	36.0	32.7					L78	46.8	27.5		24.9	26.8	
N13	39.8						T79	71.4	19.8				
Y14	40.3						G80						
E15							T81	72.4	21.5				
K16	32.6	26.4		29.2		42.3	W82	33.6					
F17	40.8						T83	72.5	22.3				
M18	33.4	33.1					M84	34.1	32.7				
E19	29.8	36.3					E85	31.1	35.9				
K20	32.5	26.7		29.6		44.1	G86						
M21	33.7	33.0					N87	39.5					
G22							K88	35.6	25.1		29.6		41.8
I23	36.9	27.9	17.8	11.4			L89	44.6	27.2		24.2	24.2	
N24							V90	34.0	21.5	21.1			
V25							G91						
V26	32.1	21.1	22.4				K92	33.3	24.9		29.2		42.1
K27	32.7	26.6		29.4		42.2	F93	43.7					
R28	30.8	28.2		44.4			K94	36.0	24.9		29.5		41.7
K29	32.1	25.3		29.1		42.2	R95	31.2	29.1		44.4		
L30	42.8	21.7		22.7	25.6		V96	32.2	22.9	22.9			
G31							D97	39.0					
A32	18.8						N98	38.6					
H33	29.8						G99						
D34	41.4						K100	34.3	26.8		28.9		42.7
N35	38.2						E101	32.7	38.0				
L36	42.3	26.6		28.2	21.3		L102	46.8	28.2		27.2	25.9	
K37	36.3	25.3		29.8		42.1	I103	39.5	28.1	17.5	12.3		
L38	46.3	26.9		26.3	24.0		A104	23.6					
T39	70.3	21.1					V105	36.2	22.3	22.3			
I40	40.5	28.5	17.2	12.0			R106	34.4	29.1		42.2		
T41	71.6	21.7					E107	34.8	36.3				
Q42	33.5	33.7					I108	37.7	26.9	17.5	12.6		
E43	31.1	36.5					S109	63.8					
G44							G110						
N45	39.5						N111	39.5					
K46	34.7	25.2		28.7		42.1	E112	33.3	37.7				
F47	43.1						L113	45.5	27.4		24.3	24.8	
T48	70.6	20.5					I114	39.5	28.2	18.5	14.3		
V49	34.7	21.6	21.6				Q115	30.8	36.3				
K50	35.3	25.0		29.5		42.1	T116	70.3	21.4				
E51	36.3	38.1					Y117	43.4					
S52	65.3						T118	70.9	21.3				
S53	67.7						Y119	43.6					
N54	40.0						E120	29.1	36.3				
F55	41.0						G121						
R56	32.4	26.9		43.4			V122	32.9	21.8	21.8			
N57	41.1						E123	33.8	37.9				
I58	43.4	27.4	18.1	14.2			A124	24.4					
D59	42.7						K125	38.1	26.1		29.8		42.2
V60	34.4	21.4	21.3				R126	33.6	29.8		43.2		
V61	34.5	21.1	21.1				I127	40.4	28.3	17.1	12.0		
F62	41.2						F128	43.1					
E63	32.9	37.0					K129	36.3	25.9		29.7		42.3
L64	41.4	26.9		26.5	23.4		K130	33.6	24.9		29.0		42.5
G65							E131	31.9	37.7				
V66	23.0	21.1	21.4										

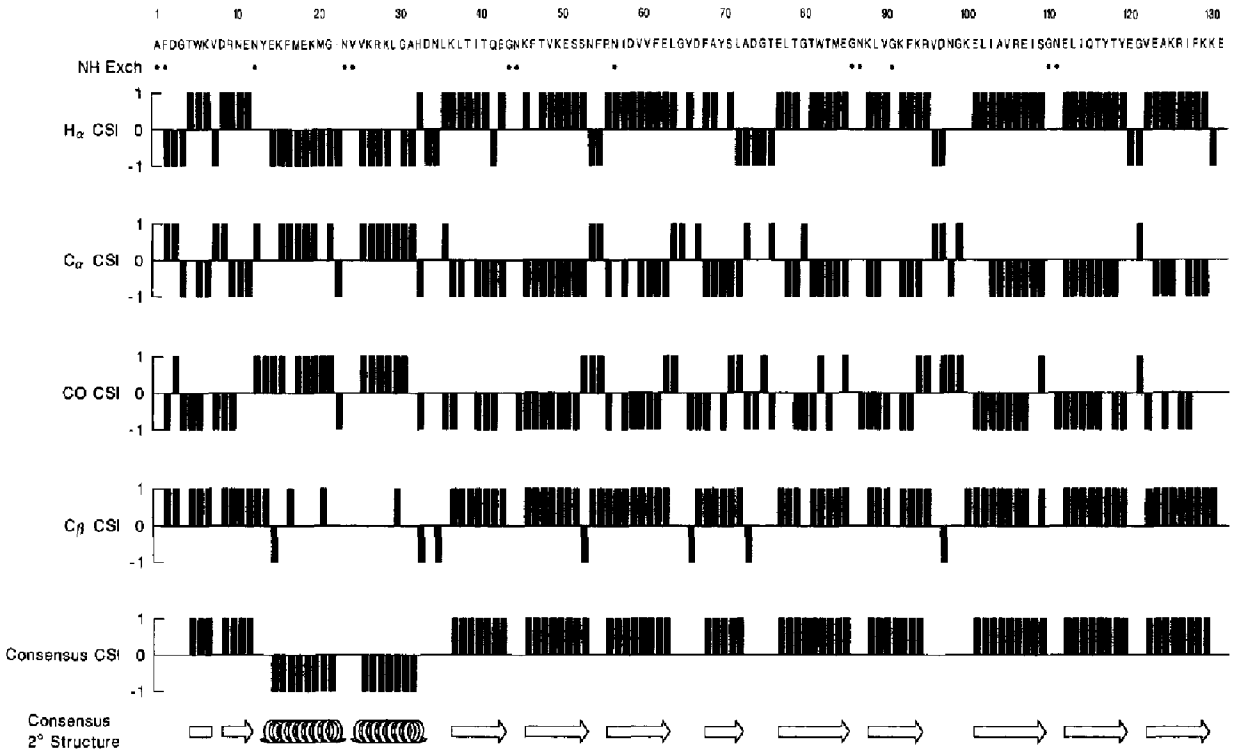

Fig. 8. Chemical shift indices (CSI) and solution secondary structure for I-FABP. The positions of the 13 rapidly exchanging amide protons are designated by filled circles.

Assignment summary

The ^{1}H, ^{13}C and ^{15}N assignments for I-FABP are listed in Tables 3–5. Figure 7 illustrates the continuity of the spectral connectivities used to assign the backbone atoms and indicates the presence or absence of correlations for each residue. Complete backbone and side-chain aliphatic ^{1}H and ^{13}C assignments have been established for 124 out of the 131 amino acids in I-FABP. Backbone atom assignments have been completely established for all except 13 residues. Seven of the 13 residues lack only the amide ^{1}H and ^{15}N resonances and are otherwise completely assigned. The remaining six residues are unassigned. Completion of the remaining assignments appears to be limited by the absence of these 13 amide ^{1}H resonances. Most likely, the missing amide protons are in rapid exchange with solvent at pH 7.2 and 37 °C and were eliminated by the use of water presaturation.* Future use of the gradient-enhanced versions of these NMR experiments will possibly recover some or all of these missing signals.

I-FABP is the first member of the lipid-binding protein family for which triple-resonance NMR approaches have been used and for which ^{13}C assignments have been established. However, assignments of only the protons have been reported for bovine heart fatty acid-binding protein (Lücke et al., 1992) and $^{1}H/^{15}N$ assignments for cellular retinoic acid-binding protein-I (Rizo et al., 1994).

Chemical shift-based determination of the solution secondary structure of I-FABP

Wishart and co-workers have recently established a chemical shift index (CSI) to quantitate the relationship between the chemical shift values for a residue and its local secondary structure (Wishart and Sykes, 1994). Using their public-domain program, individual CSI values were calculated for the $^{1}H^{\alpha}$, $^{13}C^{\alpha}$, $^{13}C^{\beta}$ and ^{13}CO atoms, and a consensus CSI was determined (Fig. 8). The solution secondary structure of I-FABP, based upon this consensus CSI, is schematically illustrated at the bottom of the figure. Overall, the solution secondary structure determined by this method agreed well with that determined by X-ray crystallography (Sacchettini et al., 1989). The only differences were seen at the edges of the secondary structure elements. The exact positions of the initiation and termination points differed by one or two residues in about half of the elements, regardless of whether the secondary structure was defined by visual inspection of the crystal structure (as in Sacchettini et al. (1989)) or by the program PROCHECK. Uncertainties of this nature are a common feature of secondary structure determination and may reflect a current lack of consensus on the precise location of these structural elements, rather

*Although the missing amide protons might have been observed by collecting spectra at pH 3–4, we deliberately chose a pH value of 7.2, not only because of its physiological relevance, but also because we hope to make direct comparisons between NMR results and calorimetric binding data performed at the same pH. In addition, the solubility of I-FABP is low at pH values between 4 and 7, since its pI is ~5.5.

than an error in the determination or a real difference between the NMR and X-ray structures.

The positions of the 13 missing amide protons are indicated by dots in Fig. 8. In general, these positions correspond to the edges of secondary structure elements in I-FABP. As these amide protons are more likely to be solvent-exposed and not involved in intramolecular hydrogen bonds, their positions are consistent with the hypothesis that they are unobservable because of rapid exchange with solvent at pH 7.2 and 37 °C (vide supra).

Future directions

The next phase of this work involves assignment of the aromatic atoms and the bound ligand, which is being performed in conjunction with the 3D solution structure determination. In addition, the assignments are being used to assess the effect of bound ligand on backbone mobility and protein stability. These detailed structural and dynamical analyses should provide further insights into the nature of ligand–protein recognition.

Acknowledgements

The authors are indebted to Dr. Changguo Tang for assistance in the testing and implementation of pulse sequences, and to Dr. Lewis Kay (University of Toronto) for providing source code and valuable advice for several of the pulse sequences employed. We also thank William Hutton (Monsanto Corporate Research) for collecting preliminary P.COSY and NOESY spectra that helped to establish the feasibility of this project. Finally, we thank Dr. Prashanth Darba and Molecular Simulations, Inc., for allowing us to participate in the interactive development of assignment tools in NMR COMPASS. This work was supported by Grants from the National Science Foundation (MCB-9205665), the American Digestive Health Foundation, and by institutional start-up funds. The Unity-500 spectrometer was supported in part by the Markey Center for Research in the Molecular Biology of Disease at Washington University. The Unity-600 machine, housed in the Washington University High-Resolution NMR Facility, was supported in part by NIH Biomedical Research Support Shared Instrument Grants LRR02004 and RR05018. D.P.C. is a Johnson & Johnson/Merck Research Scholar of the American Digestive Health Foundation.

Note added in proof

The assignments for Gly^{91} were established after this paper was accepted for publication. This updated information is included in Table 3, but not in other parts of the text and figures.

References

Banaszak, L.B., Winter, N., Xu, Z., Bernlohr, D.A., Cowan, S. and Jones, T.A. (1994) *Adv. Protein Chem.*, **45**, 89–151.

Bass, N.M. (1993) *Mol. Cell. Biochem.*, **123**, 191–202.

Bax, A., Clore, G.M. and Gronenborn, A.M. (1990a) *J. Magn. Reson.*, **88**, 425–431.

Bax, A., Ikura, M., Kay, L.E., Torchia, D.A. and Tschudin, R. (1990b) *J. Magn. Reson.*, **86**, 304–318.

Bodenhausen, G. and Ruben, D.J. (1980) *Chem. Phys. Lett.*, **69**, 185–189.

Cistola, D.P., Sacchettini, J.C., Banaszak, L.J., Walsh, M.T. and Gordon, J.I. (1989) *J. Biol. Chem.*, **264**, 2700–2710.

Farmer II, B.T., Venters, R.A., Spicer, L.D., Wittekind, M.G. and Müller, L. (1992) *J. Biomol. NMR*, **2**, 195–202.

Glatz, J.C. and Van der Vusse, G.J. (1990) *Mol. Cell. Biochem.*, **98**, 247–251.

Haunerland, N.H., Jacobson, B.L., Wesenberg, G., Rayment, I. and Holden, H. (1994) *Biochemistry*, **33**, 12378–12385.

Ikura, M., Kay, L.E. and Bax, A. (1990) *Biochemistry*, **29**, 4659–4667.

Jakoby, M.G., Miller, K.R., Toner, J.J., Bauman, A., Cheng, L., Li, E. and Cistola, D.P. (1993) *Biochemistry*, **32**, 872–878.

Kaikaus, R.M., Bass, N.M. and Ockner, R.K. (1990) *Experientia*, **46**, 617–630.

Kay, L.E., Ikura, M., Tschudin, R. and Bax, A. (1990) *J. Magn. Reson.*, **89**, 496–514.

Kay, L.E., Ikura, M., Grey, A.A. and Muhandiram, D.R. (1992) *J. Magn. Reson.*, **99**, 652–659.

Kay, L.E. (1993) *J. Magn. Reson. Ser. B*, **101**, 110–113.

Levy, G.C. and Lichter, R.L. (Eds.) (1979) *Nitrogen-15 Nuclear Magnetic Resonance Spectroscopy*, Wiley, New York, NY.

Li, E., Locke, B., Yang, N.C., Ong, D.E. and Gordon, J.I. (1987) *J. Biol. Chem.*, **262**, 13773–13779.

Li, E., Qian, S., Winter, N., d'Avignon, A., Levin, M.S. and Gordon, J.I. (1991) *J. Biol. Chem.*, **266**, 3622–3629.

Lowe, J.B., Sacchettini, J.C., Laposata, M., McQuillan, J.J. and Gordon, J.I. (1987) *J. Biol. Chem.*, **262**, 5931–5937.

Lücke, C., Lassen, D., Kreienkamp, H.-J., Spener, F. and Rüterjans, H. (1992) *Eur. J. Biochem.*, **210**, 901–910.

Marion, D., Driscoll, P.C., Kay, L.E., Wingfield, P.T., Bax, A., Gronenborn, A.M. and Clore, G.M. (1989) *Biochemistry*, **28**, 6150–6156.

Messerle, B.A., Wider, G., Otting, G., Weber, C. and Wüthrich, K. (1989) *J. Magn. Reson.*, **85**, 608–613.

Patt, S.L. (1992) *J. Magn. Reson.*, **96**, 94–102.

Powers, R., Gronenborn, A.M., Clore, G.M. and Bax, A. (1991) *J. Magn. Reson.*, **94**, 209–213.

Rizo, J., Liu, Z.-P. and Gierasch, L.M. (1994) *J. Biomol. NMR*, **4**, 741–760.

Sacchettini, J.C., Gordon, J.I. and Banaszak, L.B. (1989) *J. Mol. Biol.*, **208**, 327–339.

Shaka, A.J., Keeler, J., Frenkiel, T. and Freeman, R. (1983) *J. Magn. Reson.*, **52**, 335–338.

Shaka, A.J., Barker, P.B. and Freeman, R. (1985) *J. Magn. Reson.*, **64**, 547–552.

Shaka, A.J., Lee, C.J. and Pines, A. (1988) *J. Magn. Reson.*, **77**, 274–293.

States, D.J., Haberkorn, R.A. and Ruben, D.J. (1982) *J. Magn. Reson.*, **48**, 286–292.

Veerkamp, J., Peeters, R.A. and Maatman, R.G.H.J. (1991) *Biochim. Biophys. Acta*, **1081**, 1–24.

Wishart, D.S. and Sykes, B.D. (1994) *J. Biomol. NMR*, **4**, 171–180.